

# Phase Separation of Intrinsically Disordered Protein Polymers Mechanically Stiffens Fibrin Clots

Ivan Urosev, Joanan Lopez Morales, and Michael A. Nash\*

Fibrin (Fb) networks self-assemble through the coagulation cascade and serve as the structural foundation of blood clots. Following severe trauma or drug therapy, reduced integrity of Fb networks can lead to formation of clots with inadequate mechanical properties. A key feature of therapeutic interventions for hemostasis is therefore the ability to restore mechanical strength to clots formed under coagulopathic conditions. Here, an intrinsically disordered protein based on an elastin-like polypeptide (ELP) sequence is described, which specifically binds Fb and modulates its mechanical properties. Hemostatic ELPs (hELPs) are designed containing N- and C-terminal peptide tags that are selectively recognized by human transglutaminase factor XIIIa and covalently linked into fibrin networks via the natural coagulation cascade. Phase separation of hELPs above their lower critical solution temperature leads to stiffening and rescue of clot biophysical properties under simulated conditions of dilutive coagulopathy. In addition to phase-dependent stiffening, the resulting hELP-Fb networks exhibit resistance to plasmin degradation, reduced pore sizes, and accelerated gelation rate following initiation of clotting. These results demonstrate the ability of protein-based phase separation to modulate the physical and biochemical properties of blood clots and suggest protein phase separation as a new mechanism for achieving hemostasis in clinical settings.

In cases of severe bleeding, clotting factors are rapidly depleted at the site of injury leading to a condition known as trauma-induced coagulopathy (TIC) in as many as 25% of trauma patients with an associated increase in mortality.<sup>[4,5]</sup> To date, there are few reports of intravenous hemostatic agents that can be infused systemically to treat inaccessible or uncompressible injury sites. Current standards of care involve transfusion of blood products such as frozen plasma or platelets, or the administration of clotting proteins, but these approaches are hampered by drawbacks such as high cost, short shelf life, limited efficacy, and special storage requirements.<sup>[6,7]</sup>

Hemostasis occurs in two phases, the primary phase of which involves activation and aggregation of circulating platelets at the injury site, forming a platelet plug. In the secondary phase, fibrin (Fb) is polymerized, forming an insoluble protein hydrogel (i.e., clot) that provides structural support and hinders blood flow.<sup>[8]</sup> In this secondary phase, Fb networks form when

activated thrombin cleaves fibrinopeptides from the precursor protein fibrinogen (Fg), revealing sequences known as knobs A and B. The knobs noncovalently bind to sites referred to as holes A and B on the distal ends of neighboring Fb/Fg, allowing Fb to self-associate in a half-staggered conformation and form protofibrils. These protofibrils then bundle together to form fibers and eventually an insoluble Fb network.<sup>[9,10]</sup> Fb networks are subsequently stabilized through covalent cross-links formed by a reaction between lysine and glutamine residues catalyzed by activated clotting-associated transglutaminase, factor XIIIa (FXIIIa).<sup>[11]</sup> Fb and FXIIIa are therefore both important players in hemostasis and represent valid molecular targets for hemostatic control systems.


Targeting Fb with synthetic systems is challenging because of the difficulty in obtaining specific high-affinity binders that discriminate between gelled Fb and circulating Fg. Since Fb clots and soluble Fg share sequence and structural homology, there are only a small number of conformational epitopes that can serve as a basis for molecular discrimination.<sup>[12]</sup> Nonetheless, phage display has been used successfully to isolate Fb-specific binders.<sup>[13,14]</sup> This has led to the development of Fb-targeting hemostats based on grafting Fb-binding peptides or nanobodies onto synthetic polymers or particles that bind Fb and support clot formation *in vivo*.<sup>[15–17]</sup>

## 1. Introduction

Severe trauma is a major cause of death among individuals 45 years of age and younger, and is projected to account for as many as 8.4 million deaths per year in 2020. A plurality of these deaths are caused by failure to achieve hemostasis.<sup>[1–3]</sup>

I. Urosev, J. Lopez Morales, Prof. M. A. Nash  
Department of Chemistry  
University of Basel  
Basel 4058, Switzerland  
E-mail: michael.nash@unibas.ch

I. Urosev, J. Lopez Morales, Prof. M. A. Nash  
Department of Biosystems Science and Engineering  
ETH Zurich, Basel 4058, Switzerland

 The ORCID identification number(s) for the author(s) of this article can be found under <https://doi.org/10.1002/adfm.202005245>.

© 2020 The Authors. Published by Wiley-VCH GmbH. This is an open access article under the terms of the Creative Commons Attribution-NonCommercial-NoDerivs License, which permits use and distribution in any medium, provided the original work is properly cited, the use is non-commercial and no modifications or adaptations are made.

The copyright line for this article was changed on 7 October 2020 after original online publication.

DOI: 10.1002/adfm.202005245

Here, we present an alternative novel mechanism for specifically targeting Fb and supporting clot formation using phase separation of elastin-like polypeptides (ELPs). ELPs are intrinsically disordered protein polymers derived from the hydrophobic domain of the human extracellular matrix protein tropoelastin. ELPs comprise repetitive VPGXG pentapeptides, where X can be any amino acid excluding proline.<sup>[18]</sup> ELPs are widely used as drug delivery vehicles, components of hydrogels for tissue repair, monodisperse mechano-linkers in single-molecule experiments, and as components in protein purification and biomarker detection.<sup>[19–25]</sup> A key advantage of ELP-based molecular systems over other natural and synthetic polymers is that they are produced by genetic engineering, and therefore precisely programmable at the DNA/amino acid level with no polydispersity.<sup>[21]</sup> ELPs are intrinsically disordered proteins and undergo stimuli-responsive phase separation into protein-rich coacervates at temperatures above their lower critical solution temperature (LCST). This process is driven by dehydration of the ELP,<sup>[26–28]</sup> and is tunable based on the length and composition of the ELP sequence.<sup>[29]</sup>

Evidence is emerging that phase separation is an important phenomenon in biology, commonly employed by cells to regulate RNA catalysis, modulate gene transcription, and control signaling.<sup>[30–32]</sup> In this context, ELPs are an ideal model system for studying and controlling molecular systems using phase separation. The phase transition of ELPs can modulate properties of synthetic materials, for example, controlling the optical density and mechanical strength of hybrid PEG hydrogels.<sup>[33,34]</sup> Recently, ELP phase separation was used for mRNA sequestration and gene expression control in artificial protocells.<sup>[35]</sup> ELP phase separation has also been used to modulate properties of ELP-hybrid hydrogels.<sup>[36]</sup> For example, Wang et al. described

hyaluronic acid-bound ELPs which formed a secondary network upon coacervation, thereby strengthening HA gels.<sup>[37]</sup>

Here, we designed and produced fibrin-binding hemostatic ELPs (hELPs) by introducing glutamine and lysine residues at the N- and C-terminal ends of an ELP. Glutamine residues were embedded within a contextual sequence motif that was efficiently recognized by the clotting factor FXIIIa.<sup>[38]</sup> This design enabled enzyme-mediated covalent integration of hELP polymers into Fb networks catalyzed by FXIIIa. When introduced into Fb clots in vitro at physiological temperature, hELP-rich coacervates imparted significant enhancement in clot strength, resistance to perfusion, accelerated gelation following onset of clotting, and extended clot persistence in the presence of plasmin. hELPs lacking FXIIIa substrate tags or hELPs integrated into Fb clots below their transition temperature did not show comparable improvements in mechanical strength, indicating that both covalent integration and phase separation contribute to enhancing clot stiffness. These results demonstrate the ability of hELPs to enhance biophysical properties of blood clots through added cross-linking and phase separation. We foresee that these materials can provide a synthetic alternative or supplement to current standards of care that are based on blood product transfusion, and therefore may avoid issues that are associated with using donor derived interventions.

## 2. Results and Discussion

### 2.1. Design and Characterization of Hemostatic ELPs (hELPs)

We designed hELPs with an ABC triblock architecture (Figure 1a). The repetitive ELP component present in all three

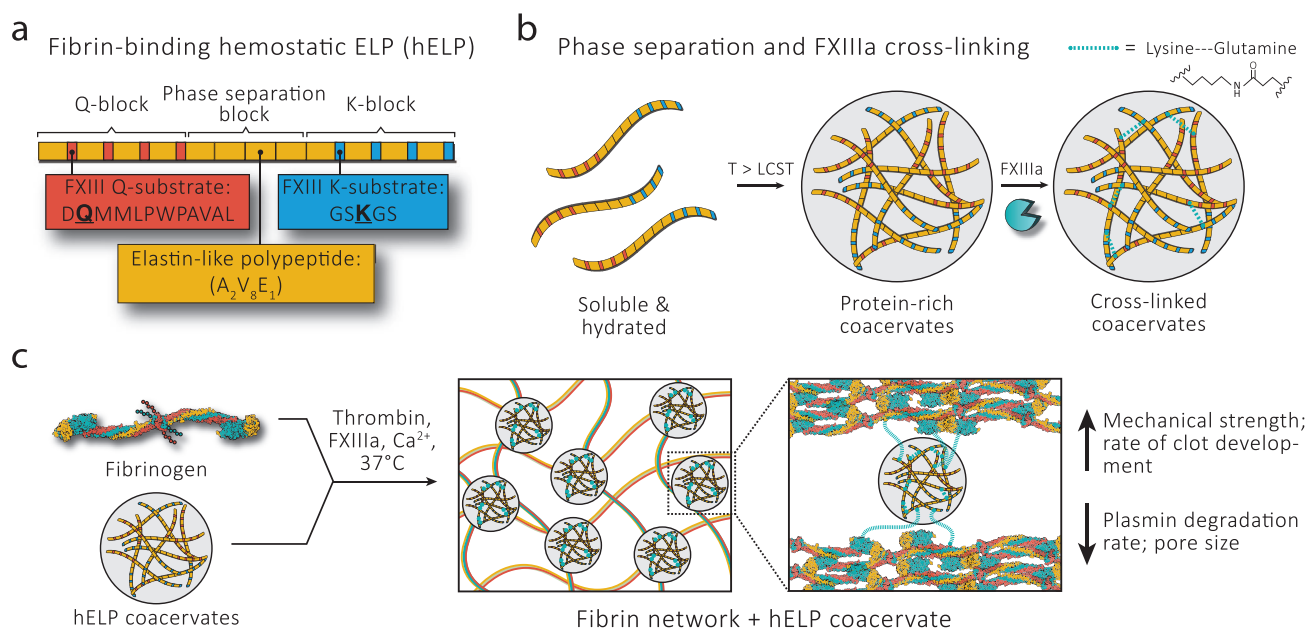


**Figure 1.** Schematic representation of hELP design, and integration into Fb clots. a) hELPs were designed as triblock copolymers containing a Q-block, a phase separation block, and a K-block. b) Above the LCST, hELPs phase separate to form coacervates, which can be covalently cross-linked by FXIIIa. c) Upon mixing with fibrinogen, thrombin and FXIII, hELP coacervates covalently integrate into Fb networks and improve mechanical strength in a phase-dependent manner, and also improve the rate of clot development following the initiation of clotting, reduce the plasmin degradation rate, and reduce the Fb network pore size. Depictions of hELPs are schematic only, and may not reflect molecular structure.

blocks comprised 11 VPGXG pentapeptides with alanine, valine, and glutamic acid residues in guest positions at a ratio of 2:8:1 ( $A_2V_8E_1$ ). Coacervation of ELPs above their LCST is accompanied by formation of ordered structures (e.g.,  $\beta$ -spirals), and reduction in solvent accessible surface area.<sup>[29]</sup> The LCST of ELPs is influenced by a number of factors, including chain length, concentration, guest residue composition, and external factors such as ionic strength and pH.<sup>[39]</sup> Based on prior literature, we designed hELPs to have an LCST slightly below physiological temperature so that coacervation was triggered when hELPs entered the physiological environment. In addition to the ELP component, the N-terminal hELP block, referred to as the Q-block, also contained four transglutaminase tags (Figure S1a, Supporting Information), each comprising a single glutamine residue embedded within a contextual sequence (DQMMLP-WPAVAL). This contextual sequence was derived from prior work<sup>[38]</sup> which used phage display to identify a glutamine donor sequence that is recognized with high efficiency by FXIIIa. By embedding these glutamine donor sequences in the broader hELP sequence, we hypothesized that hELPs would selectively integrate into Fb networks at wound sites where FXIII is activated, while avoiding off-target interactions with soluble fibrinogen.<sup>[40,41]</sup> We furthermore mutated a lysine residue within the contextual sequence to alanine (K11A), in order to eliminate the possibility of cross-links forming between Q-blocks. The middle phase separation block consisted of four consecutive  $A_2V_8E_1$  units, totaling 48 pentapeptide repeats. This block physically separated the Q- and K-blocks and extended the overall length of the hELP, thereby driving the LCST below physiological temperature. The K-block followed the phase separation block at the C-terminus of hELPs and comprised four lysine-donor sequences (GSKGS), which served as the complementary partner to glutamine in the reaction catalyzed by FXIIIa. A control ELP (conELP) was also prepared with the same sequence as hELP, except that glutamine and lysine residues were mutated to glycine such that conELP was not cross-linked by FXIIIa.

We cloned, expressed and purified hELPs and conELPs by inverse transition cycling (ITC), and measured LCSTs using a cloud point assay.<sup>[42]</sup> At a working concentration of  $30 \times 10^{-6}$  M, both hELP and conELP exhibited cloud points below 37 °C (32.7 and 34.1, °C respectively), indicating that both ELPs were aggregated at physiological temperature (Figure 2a). Next, we confirmed the functionality of the Q- and K-blocks by testing the ability of FXIIIa to cross-link hELP in the absence of Fg using SDS-PAGE (Figure 2b). A reduction in intensity of the band corresponding to single hELP polymers ( $\approx 69.5$  kDa), and the appearance of bands of higher molecular weights corresponding to hELP dimers and multimers confirmed that FXIIIa was capable of cross-linking hELPs. Meanwhile, samples of conELP incubated with FXIIIa were not cross-linked. Molecular weights of hELPs and conELPs were confirmed by mass spectrometry (Figure S1, Supporting Information).

## 2.2. Integration of hELPs into Fb Networks

We N-terminally labeled hELPs and conELPs with Atto647-N-hydroxysuccinimide (red channel) and confirmed they were still cross-linked by FXIIIa (Figure S2, Supporting Information). Fluorescent-hELPs (f-hELPs) or fluorescent-conELPs

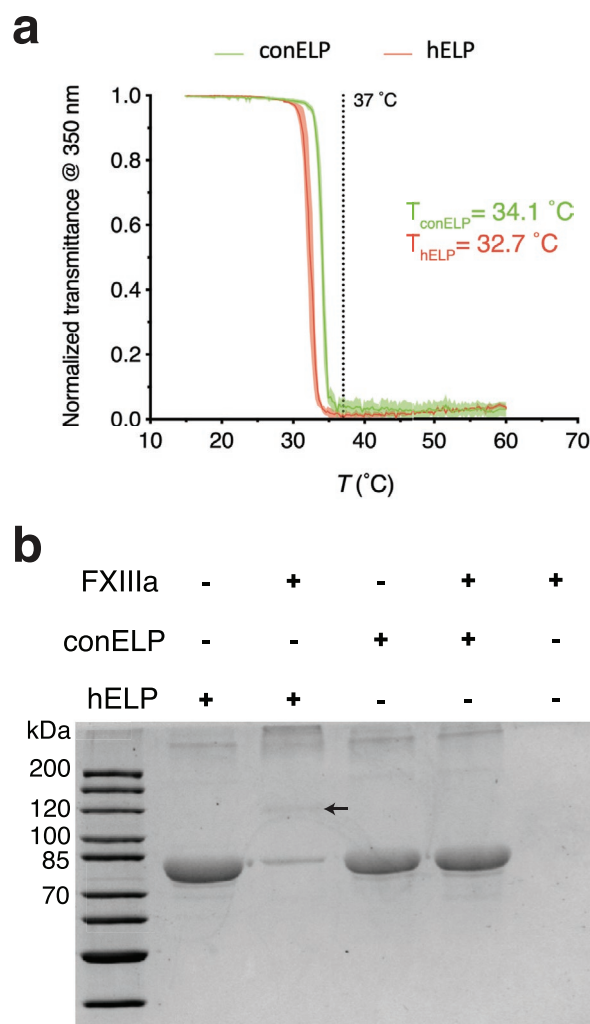


**Figure 2.** Cloud point and FXIIIa-mediated cross-linking of hELP and conELP. a) Cloud points were determined for  $30 \times 10^{-6}$  M solutions of hELP or conELP in  $20/150 \times 10^{-3}$  M HEPES/NaCl +  $20 \times 10^{-3}$  M  $CaCl_2$ . Cloud points were defined as the temperature at which normalized transmittance fell below 0.5. Data shown are mean  $\pm$  SD (shaded area) ( $n = 2$ ). b) SDS-PAGE gel following incubation of  $50 \times 10^{-6}$  M hELP or conELP with  $10 \mu\text{g mL}^{-1}$  human FXIIIa for 1 h at 37 °C. The arrow indicates the position corresponding to hELP dimers.

(f-conELPs) were then integrated into Fb clots spiked with 1% AlexaFluor 488-labeled fibrinogen (Fg-488, green channel). We used two color confocal fluorescence microscopy to characterize hELP and Fb network morphology, degree of hELP and Fb colocalization, and the influence of hELP phase transition on clot architecture. At 22 °C, all three clots (HEPES-Fb, conELP-Fb, and hELP-Fb) resulted in well-defined Fb networks when imaged in the green Fb channel (Figure 3a, left). When imaged in the red hELP channel, f-hELP fluorescence similarly showed an ordered network with high degree of spatial colocalization between hELP and Fb signals (Figure 3a, left, hELP). We observed little to no fluorescence intensity in the red channel when only HEPES buffer or f-conELP were added during formation of Fb networks (Figure 3a, left, HEPES and conELP).

To quantify hELP and Fb spatial colocalization, we used Coloc2 in ImageJ to calculate Pearson's correlation coefficients (PCC).<sup>[43]</sup> For f-hELP-Fb clots at 22 °C, a PCC between f-hELP

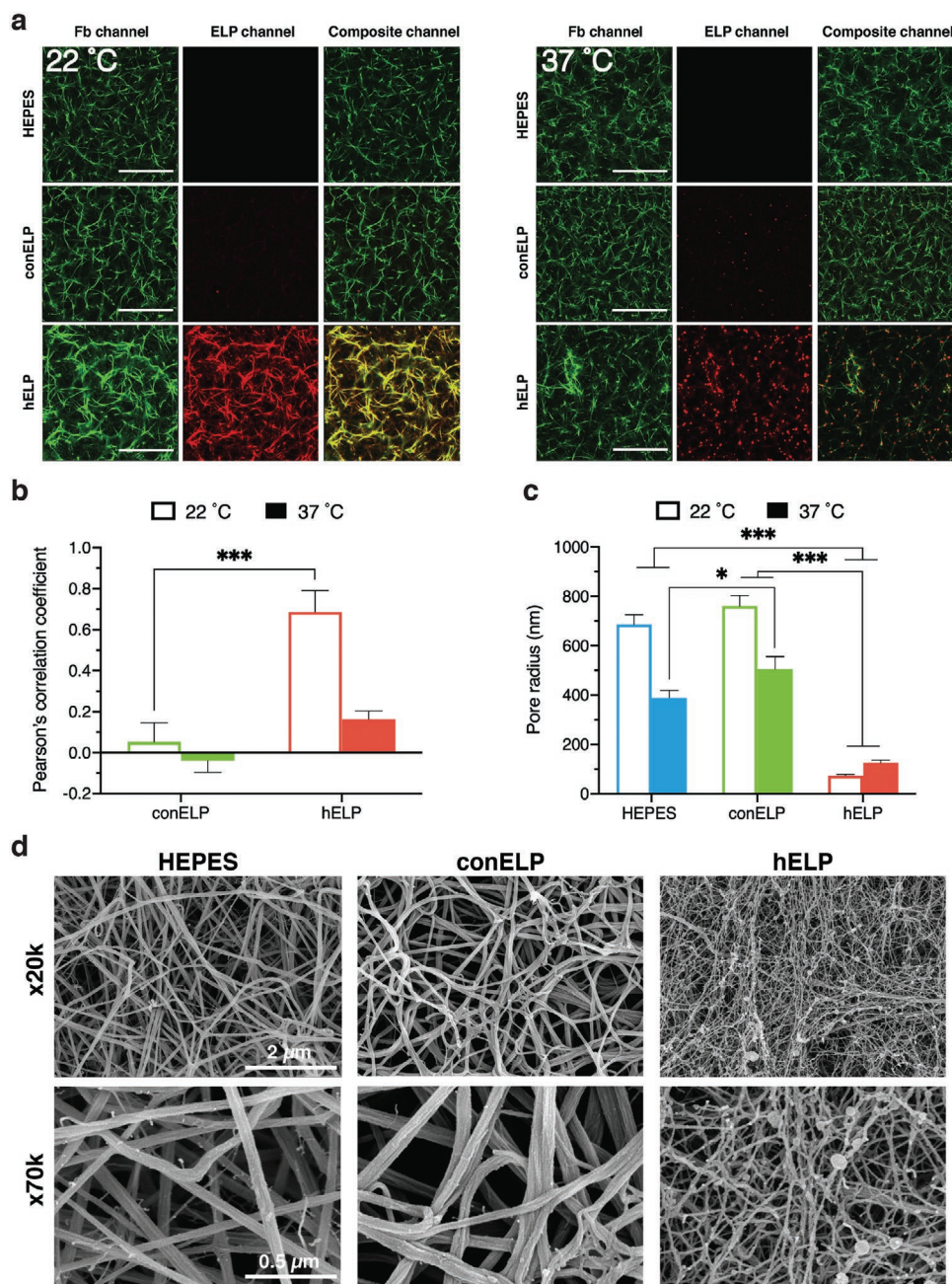


**Figure 3.** Characterizing structural morphology of hELP-Fb clots. a) Two color confocal fluorescence microscopy of  $1.5 \text{ mg mL}^{-1}$  Fb clots formed at 22 or 37 °C, with  $30 \times 10^{-6} \text{ M}$  f-conELP,  $30 \times 10^{-6} \text{ M}$  f-hELP or HEPES buffer as additives. Scale bars are 30  $\mu\text{m}$ . b) Comparison of Pearson's correlation coefficients quantifying spatial colocalization of signals from the Fb (green) or ELP (red) channels in confocal fluorescence images. c) Pore sizing of  $1.5 \text{ mg mL}^{-1}$  Fb clots containing  $30 \times 10^{-6} \text{ M}$  hELP,  $30 \times 10^{-6} \text{ M}$  conELP, or HEPES buffer. d) SEM images of  $1.5 \text{ mg mL}^{-1}$  Fb clots formed at 37 °C, with HEPES,  $30 \times 10^{-6} \text{ M}$  conELP or  $30 \times 10^{-6} \text{ M}$  hELP as additives. Images were taken at 20 000 and 70 000 $\times$  magnifications. Statistical significance in panels (b) and (c) was determined using one-way analysis of variance (ANOVA) with Tukey's post hoc test. \* $P < 0.05$  and \*\*\* $P < 0.001$ . All data in panels (b) and (c) are shown as mean  $\pm$  SD ( $n = 3$ ).

and Fb channels of  $0.69 \pm 0.1$  indicated high spatial correlation. For f-conELP-Fb clots, a PCC value of  $0.05 \pm 0.09$  indicated no spatial correlation (Figure 3b). These results demonstrate that when hELP is mixed with Fb and FXIIIa below the LCST, it is specifically cross-link and localizes to Fb fibers.

At 37 °C, above the hELP LCST (Figure 3a, right), the structures observed in conELP-Fb and hELP-Fb clots were consistent

with the expected phase separation. Punctate spots of high ELP density indicated the formation of ELP-rich coacervates at  $T > \text{LCST}$ . The density of ELP-rich coacervates was greater in f-hELP-Fb clots than in f-conELP-Fb clots due to conELPs lacking the Q and K residues required for covalent integration. F-hELP coacervates were not randomly distributed relative to the Fb network, exhibiting some colocalization with Fb

fibrils. Image analysis of hELP-Fb clots at 37 °C yielded a PCC value of  $0.163 \pm 0.04$ . For f-conELP-Fb clots formed at 37 °C, we measured a PCC value of  $-0.04 \pm 0.06$ , indicating no spatial correlation. The average diameter of hELP coacervates was determined from threshold images of three separate clots, and was found to be  $0.73 \pm 0.10 \mu\text{m}$  (Figure S3, Supporting Information). The unimodal distribution of hELP coacervate sizes with a clear central peak suggests an energy balance that caps the growth of hELP coacervates inside Fb gels. Prior work on enzymatically cross-linked ELP hydrogels<sup>[44]</sup> or enzymatic integration of ELPs into collagen networks<sup>[45]</sup> has reported that enzyme-mediated cross-linking was not inhibited above the LCST. Our results are also consistent with these findings, and indicate that coacervation did not inhibit hELP association with Fb networks. In fact, multivalent hELP-rich coacervates with locally increased concentration of Q- and K-blocks may enhance FXIIIa-mediated cross-linking.

SEM images of  $1.5 \text{ mg mL}^{-1}$  Fb clots formed at 37 °C in the presence of  $30 \times 10^{-6} \text{ M}$  ELP or HEPES buffer further highlight the structural effects hELPs have on Fb networks (Figure 3d). ConELP-Fb clots and HEPES-Fb clots both showed porous networks of thick fibers with relatively low degrees of branching. The addition of hELPs led to the formation of denser Fb networks, with thinner and more highly branched fibers. Furthermore, round aggregates bearing similarity to the coacervates observed in confocal microscopy were observed along the length of many of the fibers. The size of the putative ELP coacervates in the SEM images is significantly smaller than that determined from confocal microscopy images. We attributed this size difference to dehydration of the samples during SEM sample preparation.

FXIII is highly selective during the initial glutamine-binding step of the acyl transfer reaction, and less selective during the secondary step involving lysine recognition.<sup>[38]</sup> Typically FXIII cross-links Fb  $\gamma$ -chains into dimers, and  $\alpha$ -chains into multimers. Cross-linking of  $\gamma$ -chains is known to occur more quickly, and involves  $\gamma 406\text{K}$  on one chain linking to  $\gamma 398/399\text{Q}$  of another chain.<sup>[41,46]</sup> Cross-linking of Fb  $\alpha$ -chains by FXIII also occurs at multiple Q/K residue pairs.<sup>[41]</sup> Numerous Q- and K-residues on Fb  $\gamma$ -chains and  $\alpha$ -chains are therefore the likely sites for hELP coacervate cross-linking through the Q- and K-blocks.

The potential for hELPs to be cross-linked by other transglutaminases does exist, however, the glutamine donor sequence used in the Q-block has high specificity for human FXIII, and low reactivity with another ubiquitous transglutaminase, TGase 2.<sup>[38]</sup> Furthermore, FXIII is activated most effectively when bound to fibrin at wound sites, therefore the concentration of FXIIIa is highest at these sites, with minimal systemic concentration found in the blood. Following FXIII activation and fibrin cross-linking, both FXIII and FXIIIa are broken down by proteases released by polymorphonuclear granulocytes (PMNs), further limiting their presence in blood.<sup>[41]</sup> Based on these factors, we expect that hELP cross-linking will be localized to wound sites in vivo, and that the potential for off-target interactions of hELPs following intravenous administration is minimal.

### 2.3. Quantification of Pore Sizes

Pore size is an important architectural feature that contributes to Fb clot stiffness and resistance to enzymatic degradation.<sup>[47]</sup>

Covalent cross-linking of Fb fibrils by FXIIIa reduces pore size, while supplemental FXIIIa in vitro increases stiffness and resistance to fibrinolysis.<sup>[48,49]</sup> We investigated the effect of hELPs using a gravimetric perfusion assay where we measured liquid flow rates through hELP-Fb clots and then used Darcy's law and a model developed by Carr and Hardin<sup>[47,50]</sup> to estimate pore size.

At 22 °C, the flow rates through HEPES-Fb and conELP-Fb control clots were  $\approx 100\times$  higher than the flow rates through hELP-Fb clots (Figure S4, Supporting Information). These flow rates translated into average pore radii of  $686.6 \pm 39.3$ ,  $761.2 \pm 41.8$ , and  $73.6 \pm 5.4 \text{ nm}$  for HEPES-Fb, conELP-Fb, and hELP-Fb clots, respectively (Figure 3c). The  $\approx 10$ -fold smaller pore radius observed for hELP-Fb clots represented a significantly larger pore size reduction than previously reported for clots treated with either supplementary FXIII (a  $2.1\times$  reduction),<sup>[48]</sup> or synthetic fibrin-binding polymers (a  $1.5\times$  reduction).<sup>[47]</sup> SEM analysis of HEPES-Fb, conELP-Fb, and hELP-Fb under vacuum was also qualitatively consistent with pore size reduction (Figure 3d).

At 37 °C, pore radii in both HEPES-Fb and conELP-Fb control clots were smaller than at 22 °C ( $390.3 \pm 28.9$  and  $504.3 \pm 51.3 \text{ nm}$ , respectively), which we attributed to a temperature dependence of FXIIIa activity.<sup>[41]</sup> In hELP-Fb clots however, the pore radius at 37 °C was  $124.8 \pm 11.5 \text{ nm}$ , slightly larger but not significantly different from the radius at 22 °C (Figure 3c). An increase in temperature from 22 to 37 °C therefore did not lead to a significant change in apparent pore size as measured by gravimetric perfusion for hELP-Fb clots, as was observed in the controls. This could indicate that hELP-Fb clots are already maximally cross-linked at 22 °C.

### 2.4. Gelation Kinetics

We investigated the effect of hELPs on gelation kinetics using a turbidity assay in a UV-vis spectrophotometer (Figure 4a). Prior work has shown that the gelation of Fb clots correlates with an increase in the turbidity of the clot.<sup>[47,51,52]</sup> In our experiment, absorbance values of gelling Fb clots were measured at 350 nm over a period of 1 h at 37 °C. Several distinct gelation profiles emerged across the different groups. HEPES-Fb clots showed a brief initial lag phase of gelation, followed by a gradual increase in absorbance over a period of  $\approx 6 \text{ min}$ , after which absorbance reached a plateau at  $0.75 \pm 0.12 \text{ AU}$ s. ConELP-Fb clots had a similar initial lag phase, but this was followed by a more rapid increase in absorbance lasting approximately 45 s, after which a plateau was reached at  $0.38 \pm 0.07$ , which was significantly lower than the one seen in HEPES-Fb clots. The absorbance profile of hELP-Fb clots showed a lag phase and growth phase that were similar in length to the ones observed in conELP-Fb clots; however, hELP-Fb clots reached a significantly higher plateau absorbance of  $\approx 0.9 \pm 0.02$ .

We further measured gelation kinetics of  $2.2 \text{ mg mL}^{-1}$  Fb clots using low-strain oscillatory shear rheology under physiological conditions, focusing in particular on the shear storage ( $G'$ ) and loss ( $G''$ ) moduli. HEPES-Fb and conELP-Fb clots, an initial lag phase, was followed by a period of rapid gelation and a secondary phase of slower asymptotic growth of  $G'$  (Table 1; Figure S5, Supporting Information). The gelation time for

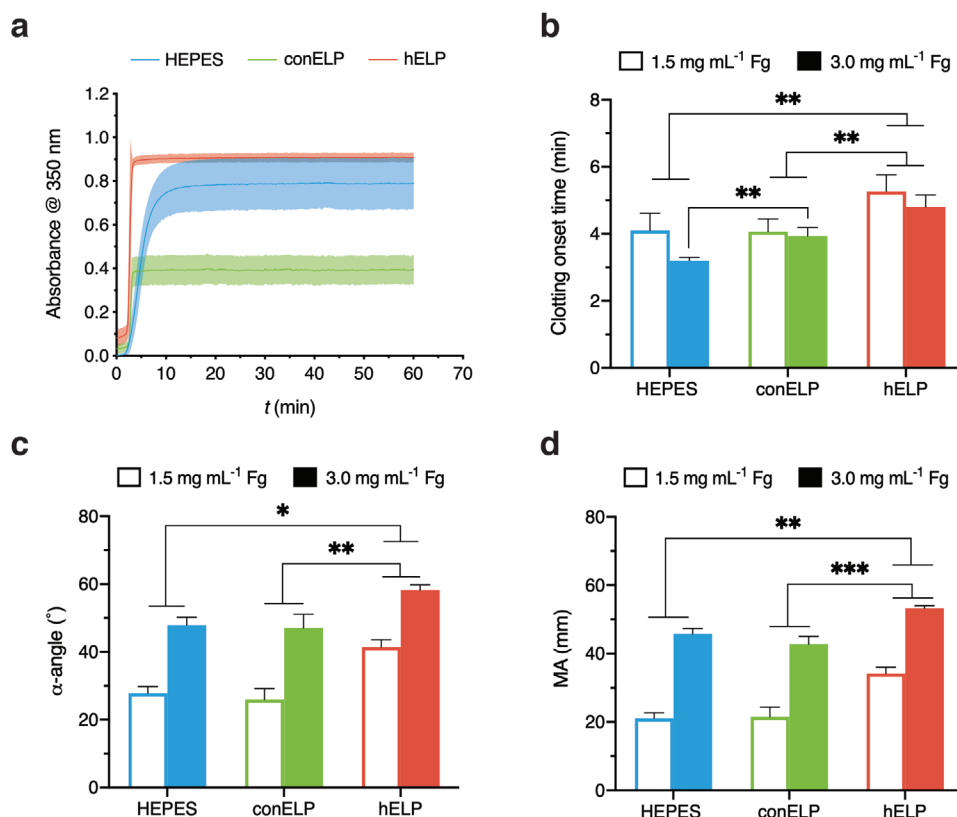


**Figure 4.** Gelation kinetics of Fb clots in the presence of hELP or conELP. a) Absorbance of gelling  $2.2 \text{ mg mL}^{-1}$  Fb clots containing  $30 \times 10^{-6} \text{ M}$  hELP, conELP, or HEPES buffer at  $37^\circ\text{C}$  at  $350 \text{ nm}$ . Measurements were taken at  $15 \text{ s}$  intervals over a period of  $1 \text{ h}$ . b) Clotting onset time ( $R$ ), c)  $\alpha$ -angle, and d) maximum amplitude (MA) of Fb clots containing  $30 \times 10^{-6} \text{ M}$  hELP, conELP, or HEPES buffer as measured by thromboelastography at  $37^\circ\text{C}$ . Data in panels (b), (c), and (d) are shown as mean  $\pm$  SD ( $n = 3$ ).  $*P < 0.05$ ,  $**P < 0.01$ , and  $***P < 0.001$ ; one-way ANOVA with Tukey's post hoc test.

conELP-Fb and HEPES-Fb clots (defined as the point where  $G' > G''$ ) occurred at  $390$  and  $330 \text{ s}$ , respectively, while the gel point for hELP-Fb clots (with  $30 \times 10^{-6} \text{ M}$  hELP) occurred significantly later at  $540 \text{ s}$ . In order to determine if steric hindrance of Fb clot formation was occurring due to high concentrations of hELP, we also performed the experiment on clots containing  $20$ ,  $10$ , and  $5 \times 10^{-6} \text{ M}$  hELP, and found that the gel point occurred earlier than controls in Fb clots with  $10 \times 10^{-6} \text{ M}$  hELP. Following onset of gelation,  $G'$  of hELP-Fb clots increased more rapidly than in HEPES-Fb or conELP-Fb clot at all hELP concentrations, however this effect was most pronounced with the addition of  $20$  and  $30 \times 10^{-6} \text{ M}$  hELP. In clinical hemostasis, Fg concentrations below  $\approx 2.3 \text{ mg mL}^{-1}$  are associated with increased mortality.<sup>[46,52]</sup> By defining the maximum  $G'$  achieved by HEPES-Fb clots over  $3600 \text{ s}$  in this experiment as the critical threshold (specifically,  $127.6 \pm 18.1 \text{ Pa}$ ), we could quantify the time required for hELP-Fb clots to reach a stiffness significantly greater than that of clots formed at this critical Fg concentration. Clots formed with  $30 \times 10^{-6} \text{ M}$  hELP exceeded this threshold after  $1860 \text{ s}$ , clots formed with  $20 \times 10^{-6} \text{ M}$  hELP did so after  $1470 \text{ s}$ , and clots formed with  $10 \times 10^{-6} \text{ M}$  hELP did so after  $2160 \text{ s}$ . ConELP-Fb clots, and clots formed with  $5 \times 10^{-6} \text{ M}$  hELP never significantly exceeded this threshold. The presence of hELP coacervates therefore had an inhibitory effect on time until initiation of clotting, but a positive effect on the subsequent rate of clot development.

## 2.5. Influence of hELPs in Thromboelastography

Thromboelastography (TEG) is a clinical technique for measuring the clotting capacity of blood, which is based on the displacement of a free-moving pin, submerged in a clotting blood sample within a rotating cup.<sup>[53]</sup> Here, we evaluated three TEG parameters, namely, reaction time ( $R$ ), which measures the time to initiation of clot formation (i.e., the time until pin displacement reaches  $2 \text{ mm}$ ),  $\alpha$ -angle which measures the rate of clot development after the  $R$  point has been reached, and maximum amplitude (MA) which measures clot stiffness in terms of the maximum displacement achieved by the pin over the

**Table 1.** Gelation kinetics parameters from rheological measurements of  $2.2 \text{ mg mL}^{-1}$  Fb clots forming at  $37^\circ\text{C}$ .

Sample	Gel point [s]	Time until $G' > G'_{2.2^a}$ [s]	Max $\frac{\partial G'}{\partial t}$ [Pa s <sup>-1</sup> ]
HEPES	330	N/A	0.08
$30 \times 10^{-6} \text{ M}$ conELP	390	N/A	0.13
$5 \times 10^{-6} \text{ M}$ hELP	480	N/A	0.14
$10 \times 10^{-6} \text{ M}$ hELP	300	2160	0.21
$20 \times 10^{-6} \text{ M}$ hELP	690	1470	0.28
$30 \times 10^{-6} \text{ M}$ hELP	540	1860	0.27

<sup>a</sup>The time until  $G'$  of sample exceeds the maximum  $G'$  of the HEPES control.

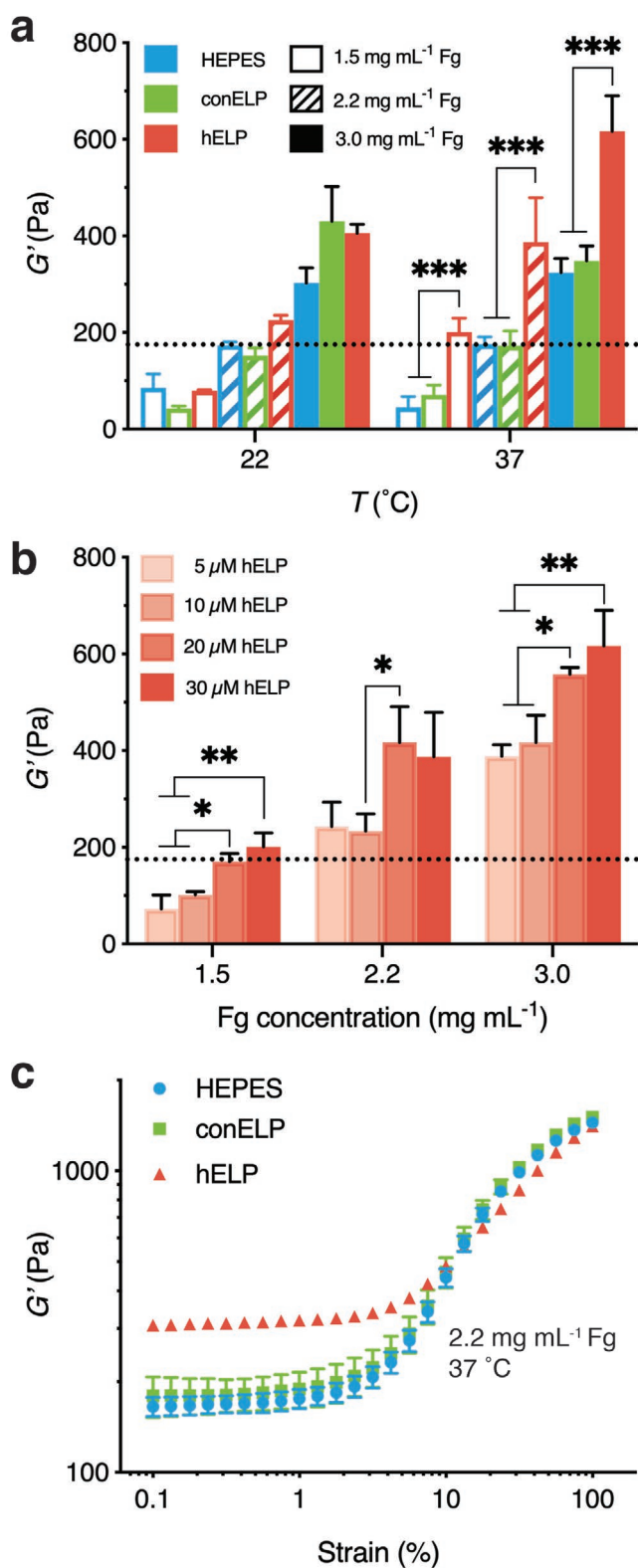


**Figure 5.** In vitro characterization of mechanical properties of hELP-Fb clots. a) Average shear storage moduli of Fb clots containing either  $30 \times 10^{-6}$  M hELP, conELP, or an equivalent volume of HEPES buffer. Gels were allowed to form between the cone and plate of the rheometer at either 22 or 37 °C, after which a frequency sweep was

performed from 0.1 to 3 Hz at 1% strain. The dotted line indicates the critical physiological threshold stiffness corresponding to the average shear storage modulus of the 2.2 mg mL<sup>-1</sup> Fb HEPES control clot. b) Average shear storage moduli of 1.5–3.0 mg mL<sup>-1</sup> Fb clots formed at 37 °C with  $(5\text{--}30) \times 10^{-6}$  M hELP as an additive. The dotted line indicates the shear storage modulus of a 2.2 mg mL<sup>-1</sup> Fb HEPES control clot. c) Strain sweeps from 0.1% to 100% ( $f = 1$  Hz) of 2.2 mg mL<sup>-1</sup> Fb gels containing  $30 \times 10^{-6}$  M hELP, conELP, or HEPES buffer at 37 °C. Data in all panels are shown as mean  $\pm$  SD ( $n = 3$ ). \* $P < 0.05$ , \*\* $P < 0.01$ , and \*\*\* $P < 0.001$ ; one-way ANOVA with Tukey's post hoc test.

course of the experiment. Here too a similar picture emerged of two phases of hELP-Fb clot formation as was observed in the turbidimetric and rheological experiments described above. The initiation of clotting required more time in hELP-Fb clots than in conELP-Fb or HEPES-Fb clots, at both low and high Fb concentrations (Figure 4b). However, following the onset of clotting, HEPES-Fb clots containing 1.5 mg mL<sup>-1</sup> Fb had a significantly higher  $\alpha$ -angle ( $41.43 \pm 2.15^\circ$ ) than HEPES-Fb or conELP-Fb controls, ( $27.83 \pm 1.95^\circ$  and  $25.93 \pm 3.26^\circ$ , respectively) (Figure 4c). When the Fb concentration was increased to 3.0 mg mL<sup>-1</sup>, the increase in  $\alpha$ -angle for hELP-Fb clots relative to controls was more modest. In this case, hELP-Fb clots had an  $\alpha$ -angle of  $58.2 \pm 1.6^\circ$  while  $\alpha$ -angles for HEPES-Fb and conELP-Fb clots were  $47.9 \pm 2.31^\circ$  and  $47.07 \pm 4.04^\circ$ , respectively. In previous studies, FXIII was found to be critical to the secondary phase of clot stiffening during gelation, and as hELPs are integrated into Fb clots by FXIII, it may be the case that their presence increases the rate of this secondary phase.<sup>[54]</sup> Therefore, while the initial onset of clotting takes longer in the presence of hELPs (as indicated by the increased  $R$  value), the subsequent rate of clot development is also increased; ultimately, the efficacy of hELPs as hemostats will depend on the interplay of these two factors in vivo.

The effect of hELPs on MA values was similar to the one observed with the  $\alpha$ -angle. For hELP-Fb clots containing  $30 \times 10^{-6}$  M hELP and 1.5 mg mL<sup>-1</sup> Fb, MA rose 62% and 59% relative to HEPES and conELP-containing clots, respectively. For hELP-Fb clots formed with 3.0 mg mL<sup>-1</sup> Fb, MA was 16% higher than HEPES-Fb clots, and 24.5% higher than conELP-Fb clots (Figure 4d). Taken together, these TEG results indicated that hELPs had a more pronounced positive effect on clot properties for clots with lower, subcritical threshold concentrations of fibrin.

## 2.6. Effect of hELP Coacervates on Fb Clot Mechanics

We used oscillatory shear rheology to measure the effect of hELPs on clot stiffness ( $G'$ ) with Fb concentrations above and below the critical Fb concentration threshold of 2.2 mg mL<sup>-1</sup>. At 22 °C, no significant differences in  $G'$  were observed at any Fb concentration for HEPES-Fb, conELP-Fb or hELP-Fb clots (Figure 5a). At 37 °C, however, we found a significant increase in  $G'$  across all Fb concentrations for hELP-Fb clots. HEPES-Fb clots with the lowest Fb concentration (1.5 mg mL<sup>-1</sup>) exhibited  $G'$  of  $201.3 \pm 16.4$  Pa, which was significantly higher than those of conELP-Fb ( $71.0 \pm 11.6$  Pa) or HEPES-Fb ( $45.0 \pm 12.8$  Pa) clots. The  $G'$  of hELP-Fb clots formed with 1.5 mg mL<sup>-1</sup> Fb was

performed from 0.1 to 3 Hz at 1% strain. The dotted line indicates the critical physiological threshold stiffness corresponding to the average shear storage modulus of the 2.2 mg mL<sup>-1</sup> Fb HEPES control clot. b) Average shear storage moduli of 1.5–3.0 mg mL<sup>-1</sup> Fb clots formed at 37 °C with  $(5\text{--}30) \times 10^{-6}$  M hELP as an additive. The dotted line indicates the shear storage modulus of a 2.2 mg mL<sup>-1</sup> Fb HEPES control clot. c) Strain sweeps from 0.1% to 100% ( $f = 1$  Hz) of 2.2 mg mL<sup>-1</sup> Fb gels containing  $30 \times 10^{-6}$  M hELP, conELP, or HEPES buffer at 37 °C. Data in all panels are shown as mean  $\pm$  SD ( $n = 3$ ). \* $P < 0.05$ , \*\* $P < 0.01$ , and \*\*\* $P < 0.001$ ; one-way ANOVA with Tukey's post hoc test.

equivalent to the  $G'$  of control clots formed at a physiological Fb concentration of  $2.2 \text{ mg mL}^{-1}$ . This indicated that at  $T > \text{LCST}$ , hELP coacervates restored clot stiffness to physiological values under simulated conditions of TIC and depleted Fg.<sup>[55]</sup>

The phase transition dependence of the stiffening effect of hELPs in Fb clots can be explained in several ways. First, the high local concentration of hELP molecules in the coacervate may promote the formation of more intermolecular hELP-hELP cross-links, establishing a secondary network. In vivo, a similar effect is observed in the phase-separation-driven formation of biomolecular condensates, wherein local concentration enhancement of substrates and enzymes can accelerate chemical reactions. This has been shown to increase rates of reaction in actin polymerization<sup>[56]</sup> and RNA catalysis, for example.<sup>[31]</sup> Secondly, aggregation of hELPs above their LCST may drive the formation of a secondary network of cross-links between Fb molecules, independent of the formation of inter-hELP cross-links. The formation of secondary networks in hydrogels by thermal assembly of ELPs was also reported by Wang et al., who showed that the aggregation of hydrazide-modified ELPs cross-linked into Hyaluronic Acid hydrogels resulted in a mechanical stiffening of those materials.<sup>[37]</sup> Finally, the phase separation of hELPs bound to Fb may exert mechanical forces on Fb fibers, creating a strain-stiffening effect even in the absence of external tension, recapitulating the active cell-driven contractile strain-stiffening that occurs in fibrin networks having imbedded fibroblasts and platelets.<sup>[57]</sup> Strain stiffening is a well-known property of Fb networks and ELP coacervation is known to stiffen ELP hydrogels and exert mechanical forces.<sup>[58–60]</sup> There is evidence that the mechanical force of molecular aggregation is applied in other contexts in vivo: Shin et al. recently showed that the phase separation of intrinsically disordered proteins associated with chromatin functions to physically pull-together distal genomic elements, while mechanically excluding others, in a mechanism that controls DNA transcription.<sup>[61]</sup> However, given that the stiffening effect is observed for hELPs that are preheated/aggregated prior to Fb polymerization, active contraction/stiffening of the network by hELP coacervates may not be a major contributor to the stiffening of hELP-Fb clots.

Additionally, we investigated how different concentrations of hELP influence the mechanical stiffening of hELP-Fb clots. Frequency sweeps were performed at  $37^\circ\text{C}$  as described above, with clots consisting of  $1.5\text{--}3.0 \text{ mg mL}^{-1}$  Fg, and  $5 \times 10^{-6}$ ,  $10 \times 10^{-6}$ ,  $20 \times 10^{-6}$ , or  $30 \times 10^{-6} \text{ M}$  hELP (Figure 5b). When the concentration of Fg was below the critical threshold, only hELP at concentrations of  $20 \times 10^{-6}$  and  $30 \times 10^{-6} \text{ M}$  were sufficient to raise the mechanical strength of clots from subcritical to threshold levels. At Fg concentrations of  $2.2 \text{ mg mL}^{-1}$ , all concentrations of hELP were able to raise the strength of clots above that of the HEPES control ( $G' = 175.0 \pm 15.5 \text{ Pa}$ ), however, the increase in stiffness was much larger for clots with  $20 \times 10^{-6}$  or  $30 \times 10^{-6} \text{ M}$  hELP ( $G' = 416.9 \pm 73.8$  and  $387.2 \pm 92.1 \text{ Pa}$ , respectively), than for clots with  $5 \times 10^{-6}$  or  $10 \times 10^{-6} \text{ M}$  hELP ( $G' = 243.2 \pm 50.4$  and  $233.4 \pm 35.4 \text{ Pa}$ , respectively). A similar pattern was observed at the highest concentration of Fg tested, where clots with  $20 \times 10^{-6}$  or  $30 \times 10^{-6} \text{ M}$  hELP had shear storage moduli of  $557.8 \pm 13.9$  and  $616.9 \pm 73.1$ , respectively, and clots formed with  $5 \times 10^{-6}$  or  $10 \times 10^{-6} \text{ M}$  hELP had shear storage moduli of  $388.2 \pm 23.9$  and  $417.2 \pm 56.1$ , respectively.

## 2.7. Influence of hELPs on Strain Stiffening of Fb Clots

Strain stiffening in Fb clots has been attributed to the multiscale structural organization of Fb networks, from single monomers, to protofibrils, to protofibril bundles, and fibers. According to this theory, as Fb networks are strained, force is first entropically dissipated by minimizing thermal fluctuations of flexible interfibril cross-links, and subsequently through the stretching of fibrils themselves. Eventually, at higher tension the secondary, tertiary, and quaternary structural elements of folded regions within Fb domains are denatured, giving rise to strain stiffening behavior that is uncommon in synthetic cross-linked polymer networks.<sup>[62,63]</sup>

To determine what effect hELPs have on Fb strain stiffening, we performed oscillatory rheology using strain ramps from 0.1% to 100% (Figure 5c). At low strains (0.1–1%), hELP-Fb clots containing  $30 \times 10^{-6} \text{ M}$  hELP and  $2.2 \text{ mg mL}^{-1}$  Fb exhibited an increase in  $G'$  as compared to conELP-Fb or HEPES-Fb clots, consistent with observations in the low amplitude frequency sweep experiments (Figure 5a). At medium (1–10%) and high strains (10–100%), all clots showed strain-stiffening behavior; however, the onset strain of the stiffening was higher for hELP-Fb ( $\approx 10\%$ ) than for conELP-Fb or HEPES-Fb clots ( $\approx 2\text{--}3\%$ ). The rate of strain stiffening was higher in HEPES-Fb and conELP-Fb clots than for hELP-Fb clots, as indicated by the maxima of the first derivative for each curve (38.1, 38.8, and  $23.1 \text{ Pa}$ , respectively). At 100% strain,  $G'$  for all clots was roughly equal ( $\approx 1400\text{--}1500 \text{ Pa}$ ). Comparing  $G'$  between 0.1% and 100% strain, hELP-Fb clots stiffened 4.6-fold, while conELP-Fb and HEPES-Fb clots stiffened 8.8- and 8.4-fold, respectively. Considering these results in the context of Fb hierarchical structure, it seems likely that by cross-linking protofibrils, hELPs minimize thermal fluctuations of unstructured regions of the network in the low strain range.<sup>[62]</sup> Once the clot is sufficiently stretched, the elastic response is dominated by stretching of individual fibers, and therefore the addition of additional cross-links in the form of hELP coacervates no longer plays a role. Previous studies have shown that supplemental FXIII increases the elastic modulus of Fb clots at low strains within the linear viscoelastic region for fibrin, but not in the nonlinear portion of the stress-strain curve, similar to what we observed here with addition of hELPs.<sup>[54]</sup>

## 2.8. Effect of hELP Coacervates on Plasminolysis

In the body, clots are enzymatically degraded by the protease plasmin, which is generated from plasminogen upon activation by tissue-plasminogen activator (tPA).<sup>[48]</sup> The proteolytic activity of plasmin is regulated spatiotemporally by binding of tPA and plasminogen to exposed cryptic binding sites on Fb clots.<sup>[64]</sup> It has previously been shown that cross-linking by FXIIIa has an inhibitory effect on fibrinolysis in vivo.<sup>[48]</sup> Since hELP coacervates are covalently integrated into Fb clots by FXIIIa, we hypothesized that hELPs could extend the lifetime of Fb clots in the presence of plasmin. To evaluate this, we performed time-lapse confocal microscopy.

Fluorescent Fb clots (formed with  $1.5 \text{ mg mL}^{-1}$  Fg) containing  $30 \times 10^{-6} \text{ M}$  hELP, conELP, or an equivalent volume of HEPES were formed in a chambered coverslip, and a solution of plasmin

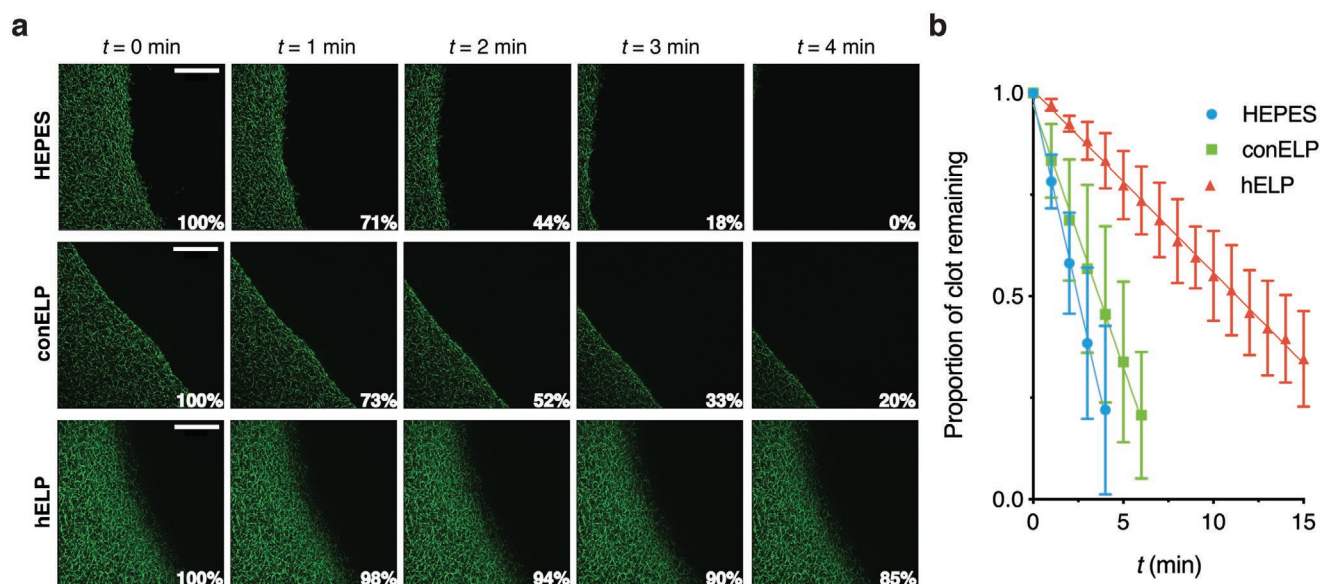


**Figure 6.** Degradation of Fb clots by plasmin. a) Time-lapse confocal images of  $1.5 \text{ mg mL}^{-1}$  Fb clots containing  $30 \times 10^{-6} \text{ M}$  hELP, conELP, or HEPES buffer, following exposure of the clot front to  $10 \mu\text{g mL}^{-1}$  plasmin at  $37^\circ\text{C}$ . Scale bars are  $60 \mu\text{m}$ . b) Quantification of the proportion of clot lysed over time for  $1.5 \text{ mg mL}^{-1}$  Fb clots containing  $30 \times 10^{-6} \text{ M}$  hELP, conELP, or HEPES buffer, as determined from confocal images of multiple clots ( $n = 3$ ).

at physiological concentration ( $10 \mu\text{g mL}^{-1}$ ) was applied to the clot front.<sup>[47]</sup> Images were taken at regular time intervals and analyzed in order to assess the proportion of clot lysed over time. Results indicated large differences in plasminolysis rates between hELP and control clots. Typically, HEPES control clots were completely degraded from the microscope field of view 4 min after the application of plasmin, whereas roughly 20% of conELP-Fb and 85% of hELP-Fb clot remained (Figure 6). The lysis rate in hELP-Fb clots was roughly three times slower than that found in conELP-Fb clots, and roughly five times slower than that found in HEPES-Fb clots. HELPs do not contain sequences recognized by plasmin,<sup>[65]</sup> therefore the additional nondegradable component in the gel inhibited fibrinolysis.

### 3. Conclusion

We report a novel mechanism for strengthening fibrin clots based on FXIIIa-mediated cross-linking and coacervation of ELPs. Our new design for hemostatic elastin-like polypeptides (hELPs) containing N- and C-terminal repetitive Q- and K-block sequences allowed them to be covalently integrated into fibrin clots via the natural clotting cascade. This approach does not require addition of cross-linking agents or bio-orthogonal functional groups, and occurs through the action of the human clotting associated transglutaminase FXIIIa. At physiological temperatures above the LCST, hELP coacervates improved the mechanical strength of fibrin clots formed under both normal and simulated coagulopathic conditions. Stiffening was not observed for fibrin networks formed in the presence of a control ELP (conELP) having nonreactive mutated FXIIIa-recognition sequences or for hELP-Fb networks formed at temperatures below LCST. This indicated that both covalent integration and phase transition of hELPs were necessary to impart clot stiffening.

HELPS were found to reduce the flow rate of buffer through fibrin clots, thereby improving the sealing properties of these materials. The addition of hELPs to Fb networks increased kinetic gelation rate following the initiation of clotting, and increased their resistance to plasmin degradation. Furthermore, hELPs were found to be noncytotoxic (Figure S6, Supporting Information). We foresee this mechanism of clot stiffening based on coacervation to be applicable in clinical settings for bleeding control, as well as in the treatment of other diseases involving components of the extracellular matrix or in the context of tissue engineering, wherein material stiffness plays an important role.

### Supporting Information

Supporting Information is available from the Wiley Online Library or from the author.

### Acknowledgements

The authors would like to thank Eva Bieler of the University of Basel Nanoimaging Institute for her assistance with acquiring SEM images. This work was supported by the University of Basel, ETH Zurich, the Swiss Nanoscience Institute, and the European Research Council (ERC Starting Grant MMA, 715207).

### Conflict of Interest

The authors declare no conflict of interest.

### Keywords

clotting, coagulation, hydrogel mechanics, protein engineering, rheology

Received: June 22, 2020

Revised: August 14, 2020

Published online: September 16, 2020

- [1] N. Curry, S. Hopewell, C. Dorée, C. Hyde, K. Brohi, S. Stanworth, *Crit. Care* **2011**, 15, R92.
- [2] C. C. Cothren, E. E. Moore, H. B. Hedegaard, K. Meng, *World J. Surg.* **2007**, 31, 1507.
- [3] C. J. Murray, A. D. Lopez, *Lancet* **1997**, 349, 1498.
- [4] K. Brohi, J. Singh, M. Heron, T. Coats, *J. Trauma: Inj., Infect., Crit. Care* **2003**, 54, 1127.
- [5] R. Davenport, J. Manson, H. De'Ath, S. Platten, A. Coates, S. Allard, D. Hart, R. Pearce, K. J. Pasi, P. MacCallum, S. Stanworth, K. Brohi, *Crit. Care Med.* **2011**, 39, 2652.
- [6] D. R. Spahn, B. Bouillon, V. Cerny, T. J. Coats, J. Duranteau, E. Fernández-Mondéjar, D. Filipescu, B. J. Hunt, R. Komadina, G. Nardi, E. Neugebauer, Y. Ozier, L. Riddez, A. Schultz, J.-L. Vincent, R. Rossaint, *Crit. Care* **2013**, 17, R76.
- [7] J. Brokloff, *J. Oral Maxillofac. Surg.* **1997**, 55, 1361.
- [8] L. W. Chan, N. J. White, S. H. Pun, *Bioconjugate Chem.* **2015**, 26, 1224.
- [9] I. N. Chernysh, C. Nagaswami, P. K. Purohit, J. W. Weisel, *Sci. Rep.* **2012**, 2, 879.
- [10] G. F. Grannis, *Clin. Chem.* **1970**, 16, 486.
- [11] A. Inbal, R. Dardik, *Pathophysiol. Haemostasis Thromb.* **2006**, 35, 162.
- [12] S. Kattula, J. R. Byrnes, A. S. Wolberg, *Arterioscler., Thromb., Vasc. Biol.* **2017**, 37, e13.
- [13] A. Putelli, J. D. Kiefer, M. Zadory, M. Matasci, D. Neri, *J. Mol. Biol.* **2014**, 426, 3606.
- [14] J. P. Yan, J. H. Ko, Y. P. Qi, *Thromb. Res.* **2004**, 114, 205.
- [15] S. Nandi, E. P. Sproul, K. Nellenbach, M. Erb, L. Gaffney, D. O. Freytes, A. C. Brown, *Biomater. Sci.* **2019**, 7, 669.
- [16] A. C. Brown, S. E. Stabenfeldt, B. Ahn, R. T. Hannan, K. S. Dhada, E. S. Herman, V. Stefanelli, N. Guzzetta, A. Alexeev, W. A. Lam, L. A. Lyon, T. H. Barker, *Nat. Mater.* **2014**, 13, 1108.
- [17] L. W. Chan, X. Wang, H. Wei, L. D. Pozzo, N. J. White, S. H. Pun, *Sci. Transl. Med.* **2015**, 7, 277ra29.
- [18] S. R. MacEwan, A. Chilkoti, *Biopolymers* **2010**, 94, 60.
- [19] K. Trabbic-Carlson, L. Liu, B. Kim, A. Chilkoti, *Protein Sci.* **2004**, 13, 3274.
- [20] M. K. McHale, L. A. Setton, A. Chilkoti, *Tissue Eng.* **2005**, 11, 1768.
- [21] S. R. MacEwan, A. Chilkoti, *J. Controlled Release* **2014**, 190, 314.
- [22] D. T. Ta, R. Vanella, M. A. Nash, *ACS Appl. Mater. Interfaces* **2018**, 10, 30147.
- [23] D. T. Ta, R. Vanella, M. A. Nash, *Nano Lett.* **2017**, 17, 7932.
- [24] W. Ott, M. A. Jobst, M. S. Bauer, E. Durner, L. F. Milles, M. A. Nash, H. E. Gaub, *ACS Nano* **2017**, 11, 6346.
- [25] W. Ott, T. Nicolaus, H. E. Gaub, M. A. Nash, *Biomacromolecules* **2016**, 17, 1330.
- [26] F. G. Quiroz, A. Chilkoti, *Nat. Mater.* **2015**, 14, 1164.
- [27] A. Valiaev, D. W. Lim, T. G. Oas, A. Chilkoti, S. Zauscher, *J. Am. Chem. Soc.* **2007**, 129, 6491.
- [28] A. Valiaev, D. W. Lim, S. Schmidler, R. L. Clark, A. Chilkoti, S. Zauscher, *J. Am. Chem. Soc.* **2008**, 130, 10939.
- [29] N. K. Li, F. G. Quiroz, C. K. Hall, A. Chilkoti, Y. G. Yingling, *Biomacromolecules* **2014**, 15, 3522.
- [30] S. F. Banani, H. O. Lee, A. A. Hyman, M. K. Rosen, *Nat. Rev. Mol. Cell Biol.* **2017**, 18, 285.
- [31] C. A. Strulson, R. C. Molden, C. D. Keating, P. C. Bevilacqua, *Nat. Chem.* **2012**, 4, 941.
- [32] Y. Shin, Y. C. Chang, D. S. W. Lee, J. Berry, D. W. Sanders, P. Ronceray, N. S. Wingreen, M. Haataja, C. P. Brangwynne, *Cell* **2018**, 175, 1481.
- [33] E. Meco, K. J. Lampe, *Biomacromolecules* **2019**, 20, 1914.
- [34] H. Wang, L. Cai, A. Paul, A. Enejder, S. C. Heilshorn, *Biomacromolecules* **2014**, 15, 3421.
- [35] J. R. Simon, S. A. Egtesadi, M. Dzuricky, L. You, A. Chilkoti, *Mol. Cell* **2019**, 75, 66.
- [36] T. Duan, H. Li, *Biomacromolecules* **2020**, 21, 2258.
- [37] H. Wang, D. Zhu, A. Paul, L. Cai, A. Enejder, F. Yang, S. C. Heilshorn, *Adv. Funct. Mater.* **2017**, 27, 1605609.
- [38] Y. Sugimura, M. Hosono, F. Wada, T. Yoshimura, M. Maki, K. Hitomi, *J. Biol. Chem.* **2006**, 281, 17699.
- [39] J. R. McDaniel, D. C. Radford, A. Chilkoti, *Biomacromolecules* **2013**, 14, 2866.
- [40] Z. Bagoly, Z. Koncz, J. Hársfalvi, L. Muszbek, *Thromb. Res.* **2012**, 129, 382.
- [41] L. Muszbek, Z. Bereczky, Z. Bagoly, I. Komáromi, É. Katona, *Physiol. Rev.* **2011**, 91, 931.
- [42] C. Boutsis, E. G. Chatzi, C. Kiparissides, *Polymer* **1997**, 38, 2567.
- [43] J. Adler, I. Parmryd, *Cytometry, Part A* **2010**, 77A, 733.
- [44] M. K. McHale, L. A. Setton, A. Chilkoti, *Tissue Eng.* **2005**, 11, 1768.
- [45] Y. Garcia, N. Hemantkumar, R. Collighan, M. Griffin, J. C. Rodriguez-Cabello, A. Pandit, *Tissue Eng., Part A* **2009**, 15, 887.
- [46] M. W. Mosesson, *J. Thromb. Haemostasis* **2005**, 3, 1894.
- [47] L. W. Chan, X. Wang, H. Wei, L. D. Pozzo, N. J. White, S. H. Pun, *Sci. Transl. Med.* **2015**, 7, 277ra29.
- [48] E. L. Hethershaw, A. L. Cilia La Corte, C. Duval, M. Ali, P. J. Grant, R. A. S. Ariens, H. Philippou, *J. Thromb. Haemostasis* **2014**, 12, 197.
- [49] O. M. Theusinger, W. Baulig, L. M. Asmis, B. Seifert, D. R. Spahn, *Thromb. Haemostasis* **2010**, 104, 385.
- [50] M. E. Carr, C. L. Hardin, *Am. J. Physiol.* **1987**, 253, H1069.
- [51] A. S. Wolberg, *Blood Rev.* **2007**, 21, 131.
- [52] E. Mihalko, A. C. Brown, *Semin. Thromb. Hemostasis* **2020**, 46, 96.
- [53] D. Whiting, J. A. DiNardo, *Am. J. Hematol.* **2014**, 89, 228.
- [54] N. A. Kurniawan, J. Grimbergen, J. Koopman, G. H. Koenderink, *J. Thromb. Haemostasis* **2014**, 12, 1687.
- [55] D. Frith, J. C. Goslings, C. Gaarder, M. Maegele, M. J. Cohen, S. Allard, P. I. Johansson, S. Stanworth, C. Thiemermann, K. Brohi, *J. Thromb. Haemostasis* **2010**, 8, 1919.
- [56] P. Li, S. Banjade, H. C. Cheng, S. Kim, B. Chen, L. Guo, M. Llaguno, J. V. Hollingsworth, D. S. King, S. F. Banani, P. S. Russo, Q. X. Jiang, B. T. Nixon, M. K. Rosen, *Nature* **2012**, 483, 336.
- [57] K. A. Jansen, R. G. Bacabac, I. K. Piechocka, G. H. Koenderink, *Biophys. J.* **2013**, 105, 2240.
- [58] D. W. Urry, B. Haynes, H. Zhang, R. D. Harris, K. U. Prasad, *Proc. Natl. Acad. Sci. USA* **1988**, 85, 3407.
- [59] D. W. Urry, B. Haynes, R. D. Harris, *Biochem. Biophys. Res. Commun.* **1986**, 141, 749.
- [60] K. Trabbic-Carlson, L. A. Setton, A. Chilkoti, *Biomacromolecules* **2003**, 4, 572.
- [61] Y. Shin, Y.-C. Chang, D. S. W. Lee, J. Berry, D. W. Sanders, P. Ronceray, N. S. Wingreen, M. Haataja, C. P. Brangwynne, *Cell* **2018**, 175, 1481.
- [62] I. K. Piechocka, R. G. Bacabac, M. Potters, F. C. MacKintosh, G. H. Koenderink, *Biophys. J.* **2010**, 98, 2281.
- [63] I. K. Piechocka, K. A. Jansen, C. P. Broedersz, N. A. Kurniawan, F. C. MacKintosh, G. H. Koenderink, *Soft Matter* **2016**, 12, 2145.
- [64] L. Medved, W. Nieuwenhuizen, *Thromb. Haemostasis* **2003**, 89, 409.
- [65] G. Cesarman-Maus, K. A. Hajjar, *Br. J. Haematol.* **2005**, 129, 307.